Measurement of dynamic full-field internal stresses through surface laser Doppler vibrometry

Stephen D. Holland,[a] Jeremy Renshaw, and Ron Roberts
Department of Aerospace Engineering and Center for Nondestructive Evaluation, Iowa State University, Ames, Iowa 50011, USA

(Received 17 July 2007; accepted 7 September 2007; published online 24 September 2007)

We present a method for evaluating internal dynamic stresses in a solid vibrating body from measurements of surface motion. The method relies on the same mathematics as boundary element method: A boundary reciprocity integral represents interior motion as a surface integral of boundary motion times the Green's function. The surface motions are measured with a laser vibrometer rather than simulated, giving a direct measurement of internal motions and internal dynamic stresses. Experimental results on a flexing beam demonstrate that stresses measured in this fashion match those calculated from elementary theory. © *2007 American Institute of Physics*.
[DOI: 10.1063/1.2790379]

In the recent years, the ability to analyze internal stresses in static objects has improved dramatically. Given measured external forces on an object, finite element calculations can accurately and reliably evaluate the internal stress and strain components.[1] The same level of progress has not been made in measuring the internal dynamic stress in vibrating bodies. There are three primary reasons for this. First, four-dimensional simulations (three spatial dimensions plus time) require so many elements and so much computation as to have been computationally infeasible until comparatively recently. Second, the wave equation becomes dispersive—a fundamental change in character—when discretized,[2] and thus simulations are inherently suspect except with extraordinarily fine meshes. Third, accurate simulations require accurate modeling of the dynamic response of the mounting apparatus, which is difficult or impossible to measure.

Several methods are available for imaging the stresses inside a vibrating body. Stress-induced photoelastic optical birefringence gives the thickness integral of the difference of principal stresses in a transparent vibrating body.[3] Utilizing the method known as stress pattern analysis by thermal emission,[4] bulk dilatation at the surface of a solid can be calculated from infrared images of the minute heating and cooling as the material compresses and expands.

Internal stresses can be estimated from the knowledge of surface motions. Our experiments use a laser vibrometer (laser Doppler velocimeter), in which the reflection of the laser spot interferes with a reference beam that has been frequency shifted using a Bragg cell. The frequency of the interference is then a direct measurement of the Doppler shift of the reflected laser light, and therefore the surface velocity parallel to the beam at the reflecting surface point can be evaluated. A variety of laser vibrometers are commercially available, including scanning and multiaxis models.

In this letter we develop and demonstrate a method for evaluating the dynamic full-field internal stress/strain state inside homogeneous solid objects through quantitative measurements of surface vibration captured with a laser vibrometer. Our method uses measurements of the full three-axis vibration across the entire boundary of an object to evaluate the motion inside the object. This is analogous to a boundary element method computation where instead of performing a simulation at the boundary, the boundary motions are actually *measured*. Our method is equivalent to a boundary element simulation where experimental measurements replace the simulation.

We evaluate internal motions from the boundary motion using a reciprocity integral formulation and the Green's function, following the logic of Achenbach.[5] The equations of motion in a solid body are

$$\sigma_{ij,i} + f_j = \rho \ddot{u}_j, \tag{1}$$

for stress tensor σ_{ij}, body force f_j, mass density ρ, and particle displacement u_j. The time-harmonic Green's function is the solution to Eq. (1) in response to a time-harmonic body force impulse in the kth direction at $x=X: f_j = \delta(\underline{x} - \underline{X}) e^{-i\omega t} \delta_{jk}$. Thus the stress and displacement Green's functions $\sigma_{ij:k}^{G:X}$ and $u_{j:k}^{G:X}$ satisfy

$$\sigma_{ij:k,i}^{G:X} + \delta(\underline{x} - \underline{X}) e^{-i\omega t} \delta_{jk} = \rho \ddot{u}_{j:k}^{G:X}, \tag{2}$$

where summation is implied by repeated indices (Einstein notation) and the comma denotes spatial differentiation with respect to the index following the comma. Note that roman i represents the imaginary number, while italic i denotes an index.

The reciprocity formulation is the equations of motion [Eq. (1)] with no body force ($f_j=0$), multiplied on both sides by the Green's function displacement $u_{j:k}^{G:X}$, and then subtracted from the Greens function equation which is itself multiplied by the specimen displacement u_j,

$$\sigma_{ij:k,i}^{G:X} u_j - \sigma_{ij,i} u_{j:k}^{G:X} = [\rho \ddot{u}_{j:k}^{G:X} - \delta(\underline{x} - \underline{X}) e^{-i\omega t} \delta_{jk}] u_j - \rho \ddot{u}_j u_{j:k}^{G:X}. \tag{3}$$

This equation is simplified, subject to the symmetries of the stiffness tensor, and integrated over the volume of the specimen. Several terms are grouped into the form of a divergence and transformed into a surface integral through the divergence theorem, yielding

[a]Electronic mail: sdh4@iastate.edu

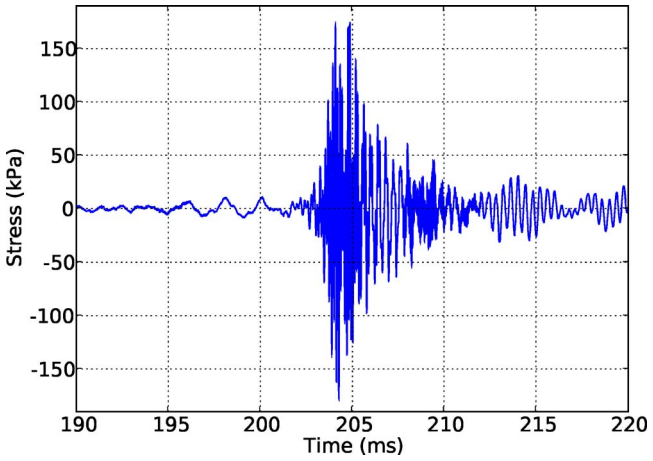

FIG. 1. (Color online) Stress as a function of time at the centroid of the bar, as measured using Eqs. (6) and (7). The excitation was a 100 Hz–20 kHz chirp between $t=200$ ms and $t=210$ ms.

$$\int_V (\delta[\underline{x}-\underline{X})e^{-i\omega t}\delta_{jk}u_j]dV = -\int_S (\sigma_{ij:k}^{G:X}u_j - \sigma_{ij}u_{j:k}^{G:X})n_i dA, \tag{4}$$

where n_i is the surface normal. The volume integral can be readily evaluated, and if the surface tractions are zero, then $\sigma_{ij}u_{j:k}^{G:X}n_i$ is also zero. The displacement at any internal point X can therefore be evaluated as

$$u_k|_{\underline{x}=\underline{X}} = \frac{1}{e^{-i\omega t}}\int_S (-\sigma_{ij:k}^{G:X}u_j)n_i dS. \tag{5}$$

Strain is the spatial derivative of displacement,

$$\epsilon_{kl} = \frac{u_{k,l}+u_{l,k}}{2} = \left.\frac{1}{i\omega e^{-i\omega t}}\int_S [(\sigma_{ij:k,l}^{G:X}+\sigma_{ij:l,k}^{G:X})v_j]n_i dS\right|_{\underline{X}=\underline{x}}, \tag{6}$$

where we have replaced u_j with $v_j/i\omega$, since velocity not displacement is our measurable quantity. The stress can be trivially calculated from the strain using Hooke's law for an isotropic medium,

$$\sigma_{ij} = 2\mu\epsilon_{ij} + \lambda\epsilon_{kk}\delta_{ik}, \tag{7}$$

where λ and μ are the Lamé stiffness constants. To summarize, given the vector surface velocity measured over the entire boundary of a solid body, we can calculate the stress everywhere within the body using Eqs. (6) and (7) and the derivatives of the well-known stress Green's function.[6]

Evaluating the internal stresses of a specimen using Eqs. (6) and (7) requires measuring the vector surface velocity over the entire boundary of the specimen. Obviously this measurement is impractical due to the need for support and mounting. Fortunately, the Green's function drops off as $1/R$ in the far field, so errors due to surfaces that cannot be measured will be primarily significant only in the immediate vicinity of those points that could not be measured.

To demonstrate this method we tested it first on a simple geometry: a $26\times13\times154$ mm^3 rectangular bar. The bar was mounted at a single point, bolted directly to a piezoelectric stack actuator, and covered with retroreflective tape. We created discrete 5×5 mm^2 tessellations of each of the five accessible faces. The bar, actuator, and laser vibrometer were mounted on carefully calibrated and aligned motion stages, so that the motion at each point on each face could be measured from different directions of incidence. The bar was repeatedly vibrated by the actuator with a 100 Hz–20 kHz frequency-swept waveform, and the laser vibrometer was scanned three times over each face at different (linearly independent) incidence directions to obtain the Cartesian velocity components needed to evaluate Eq. (6).

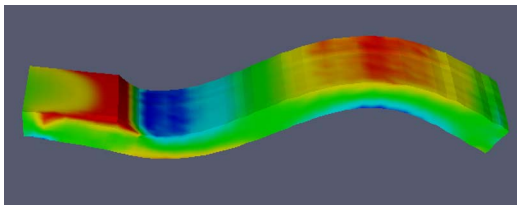

FIG. 2. (Color online) Mode shape of the 7.4 kHz resonant mode, as measured with the laser vibrometer. Bending stress σ_{xx} of this mode, measured using Eqs. (6) and (7), has been mapped to color.

Calculating the velocity or strain rate tensor at an interior point requires numerically evaluating the boundary integral of Eq. (6). The simplest solution is to replace the integral with a sum over the tessellated surface elements and evaluate the Green's function at the center of each element. This is sufficient only when the radius vector from the interior point to the center of an element is approximately equal to the radius vector to all points on the element. That is, the simple solution only works for tessellated elements that are a relatively large distance from the reference position where the internal motions are being evaluated. To work around this problem we developed an algorithm that subtessellates elements that are too close to the reference position. Once subtessellated, the element size relative to the radius is smaller, and subtessellation is repeated recursively until the far-field approximation holds.

Evaluation of Eqs. (6) and (7) in the frequency domain followed by an inverse Fourier transform gives the stress tensor as a function of time at each point inside the bar. To illustrate, the cross-sectional shear stress σ_{23} at the centroid of the bar is shown in Fig. 1. Quantitative stresses (in Pas-

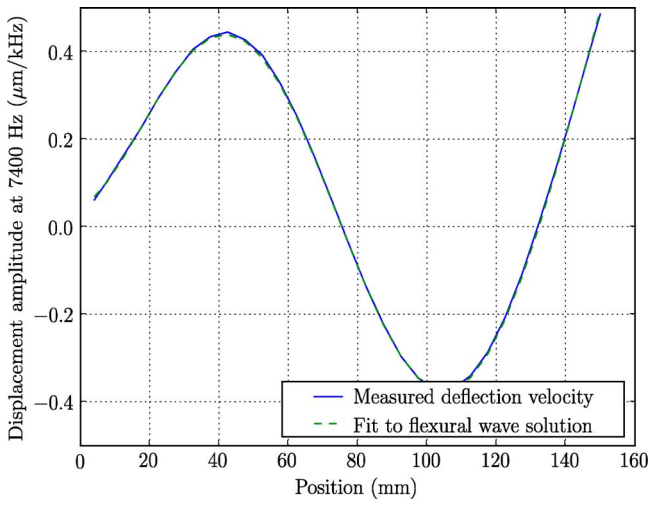

FIG. 3. (Color online) Mode profile of the 7.4 kHz resonant mode and the best-fit flexural mode shape. The curve fit is $y=-0.272\sinh(\kappa x)+0.272\cosh(\kappa x)+0.337\sin(\kappa x)-0.226\cos(\kappa x)$ μm/kHz. The two curves are almost perfectly superimposed.

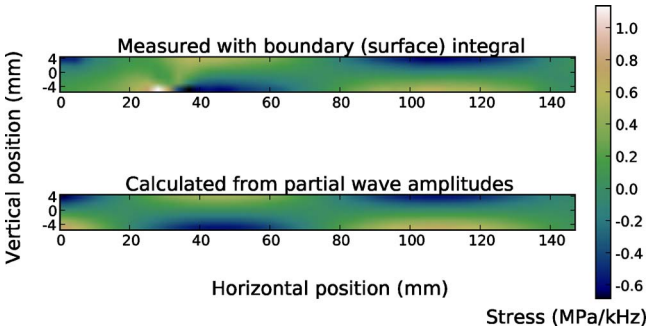

FIG. 4. (Color online) Color mapped images of the measured and calculated stresses.

cals) can be calculated anywhere in the bar except near the unmeasurable region near the transducer.

A number of resonances are observed in the measured spectra. Several of these are bending mode resonances and as such can be compared with flexural wave theory. The frequency-domain stresses calculated with Eqs. (6) and (7) can be directly compared to stresses calculated from flexural wave theory given the surface motion profile of the mode. One such mode exists at 7.4 kHz, with the mode shape shown in Fig. 2 and lengthwise displacement profile shown in Fig. 3 along with the four-parameter best fit flexural mode shape. Figure 4 shows the normal σ_{xx} bending stress distribution along a lengthwise slice of the bar as measured through Eqs. (6) and (7), as well as the same quantity calculated from flexural wave theory given the mode-shape and partial wave amplitudes of Fig. 3. Observe that the two images in Fig. 4 match almost precisely except at $x<35$ mm, where all of the points on the bottom side of the sample were shadowed by the actuating transducer and were hence unmeasurable. No additional fitting or amplitude scaling was needed to make the two parts of Fig. 4 match. Typical deviation between the two parts of Fig. 4 is approximately ±5%, except near the missing data points such as those in the unmeasurable region near the transducer. The other normal stress components at this frequency are approximately zero, as predicted by flexural wave theory.

The stress field calculated by integrating measured velocities over the boundary of the bar matches that calculated from flexural wave theory given only the partial wave amplitudes. Thus we conclude that, at least in this case, the boundary integral method described above correctly calculated the internal stresses in the bar. Due to the $1/R$ dependence of the Green's function, the effect of unmeasurable points was limited to the immediate vicinity of those points, and a close match with theory was observed everywhere outside that range.

Obviously the method as described is limited to solid, homogeneous, and isotropic solids with accessible surfaces. Known inhomogeneity or anisotropy can be taken into account through the use of alternative Green's functions that include the inhomogeneity or anisotropy. Such Green's functions can be calculated through theory or numerical computation, and would generally maintain the $1/R$ dependence and associated robustness of the Green's function in the face of missing measurement points. Unknown inhomogeneity such as a large internal flaw would act as a scatterer and appear in the observed stress field as a source of stress or stress concentration.

We have described a method for calculating dynamic internal stresses in vibrating solids from surface vibrometry measurements. The calculation relies on the Green's function and the reciprocity integral formulation to evaluate the internal motion at a point in terms of a surface integral of the motion on the boundary. The method has been demonstrated experimentally. In an example involving a bending mode, it gives an equivalent internal stress distribution to that given by flexural wave theory. Other methods of inferring dynamic internal stresses give less direct measures of the stress. Our technique allows experimental measurement and direct computation of all dynamic stress tensor components inside a vibrating solid object.

This material is based on the work supported by the Air Force Research Laboratory under Contract No. FA8650-04-C-5228 at Iowa State University's Center for NDE.

[1]S. S. Rao, *The Finite Element Method in Engineering* (Elsevier, Burlington, MA, 2005), pp. 399–420.
[2]W. R. Scott, Jr. and G. S. Warren, IEEE Trans. Antennas Propag. **42**, 1502 (1994).
[3]C. P. Burger, *Handbook on Experimental Mechanics*, edited by A. S. Kobayashi (Prentice Hall, Englewood Cliffs, NJ, 1987), pp. 260–276.
[4]R. A. Tomlinson, A. D. Nurse, and E. A. Patterson, Fatigue Fract. Eng. Mater. Struct. **20**, 217 (1997).
[5]J. D. Achenbach, *Reciprocity in Elastodynamics* (Cambridge University Press, New York, 2003), pp. 90–92.
[6]S. Kobayashi, in *Computational Methods in Mechanics*, Boundary Element Methods in Mechanics Vol. 3, edited by D. E. Beskos (North-Holland, New York, 1987), pp. 192–248.